Persistent ferromagnetism in antiferromagnetic $Pr_{0.6}Ca_{0.4}MnO_3$

N. Biškup,* A. de Andrés, and M. García Hernández
Instituto de Ciencia de Materiales de Madrid, Consejo Superior de Investigaciones Cientificas, Cantoblanco, 28049 Madrid, Spain
(Received 12 June 2008; revised manuscript received 16 September 2008; published 24 November 2008)

We report on the magnetic-field-driven persistent ferromagnetic (FM) state in antiferromagnetic (AF) manganite $Pr_{1-x}Ca_xMnO_3$, where $x=0.4$ and 0.375. At low temperatures the magnetic field-induced ferromagnetism (FIFM) persists even at $B=0$ and is quenched to a fractional value of the total number of spins. This incomplete ferromagnetism decreases with increasing temperature and disappears at $T_m=10-20$ K. T_m depends on the hole concentration "x" and increases as $x\rightarrow 0.3$. We interpret this as the incomplete relaxation from FM toward AF spin orientation, resulting in the canted antiferromagnetism (CAF). This is in contrast to the "virgin" (zero-field cooled) magnetic ground state where no ferromagnetic component could be detected. Due to the strong competition between FM and AF orders, three successive AF transitions are detected. The low-temperature transition at $T_3=27$ K has a strong influence on FIFM, resulting in the minimum magnetic field required to trigger the FIFM state. Furthermore, the $T_3=27$ K transition results in a pronounced anomaly in the temperature variation in magnetization. We comment on this property in the light of a similar finding in the phase-separated $La_{0.21}Pr_{0.42}Ca_{3/8}MnO_3$ which was interpreted as the strain-glass transition.

DOI: 10.1103/PhysRevB.78.184435 PACS number(s): 75.47.Lx, 75.50.Lk, 75.30.Cr, 75.30.Kz

I. INTRODUCTION

The transition-metal oxides, when several physical interactions—spin, charge, orbital, and lattice—act simultaneously, exhibit a large variety of physical phenomena, including high-T_C superconductivity, colossal magnetoresistance (CMR), and multiferroic behavior.[1] The complexity of the above interactions still presents a strong challenge in our understanding of these materials. In the last ten years the concept of phase separation has emerged in order to explain the CMR in mixed-valence manganites[2] and has been extended to high-T_C superconductors, such as cobaltites, ruthenates, and organic superconductors.[1,3] It is understood that in the systems with strongly competing interactions, the competing phases are spatially separated. In the mixed-valence manganites $R_{1-x}A_xMnO_3$, where $R=La,Pr,Nd,\ldots$, $A=Sr,Ca,Ba\ldots$, and $0<x<1$, the two competing phases are frequently the ferromagnetic (FM) metallic phase and the antiferromagnetic (AF) insulating phase. In this simplified view, the CMR is viewed as the percolation of current through the coalescing FM metallic domains under the influence of external magnetic field.[4,5]

The prototype CMR manganite is $Pr_{1-x}Ca_xMnO_3$ (PCMO), where $x=0.3-0.5$.[6] In this material, the charge and orbital order (CO/OO) was found more than 20 years ago[7] and was identified with the CE type of AF order. In the subsequent reports the charge ordering (CO) and AF transitions are found to be separated.[8,9] The three magnetic transitions in $\chi(T)$ are usually assigned as (a) CO ($T_{CO}=220-240$ K), (b) AF ordering ($T_N=140-180$), and (c) canted antiferromagnetic (CAF) ordering ($T_{CAF}<100$ K).[6] At low temperatures a magnetic field of several teslas is able to overturn the AF order into FM order which results in the CMR. Investigating the origin of this colossal effect, the magnetic structure was studied by neutron scattering. In $Pr_{0.7}Ca_{0.3}MnO_3$ at $B=0$ T and $T<150$ K a phase separation has been found.[10,11] The two coexisting phases, one AF charge ordered phase and another glassy nonmagnetic phase were both found to be insulating in accordance with the semiconducting behavior of the resistance. An external magnetic field overturns both phases into the almost complete (85% sample fraction) ferromagnetic delocalized (metallic) phase.[10,11]

The charge order is another conflicting point in the understanding of $Pr_{1-x}Ca_xMnO_3$ ground states. CO in manganites refers to the spatial order of Mn^{3+} and Mn^{4+} ions that are claimed to form stripes.[12–14] However, in the last several years the concept of separated charges in transition-metal oxides has been questioned.[15,16] This was initiated in 2002 by the publication of a report claiming an intermediate valence state of Mn ions in $Pr_{0.6}Ca_{0.4}MnO_3$ instead of the CO state.[17] The authors in Ref. 17 found no evidence of spatial charge ordering at $T=195<235$ K$=T_{CO}$ in their high-quality single crystal. Instead, they explain both the transport and magnetization anomalies at $T_{CO}=235$ K as the onset of ferromagnetic coupling of two adjacent Mn ions: the "Zener-polaron" ordering. The dimerization of Mn ions then changes the balance of FM and AF correlations, and the susceptibility decreases. The complex and controversial nature of electron interaction in this system is still a hotly debated issue. Recently it was reported that the Zener-polaron type of CO/OO order coexists with unordered regions even at room temperature[18] and that Zener-polaron order results in the static electric polarization.[18,19]

In order to give some more insight into the nature of ground state and competing phases of $Pr_{0.6}Ca_{0.4}MnO_3$, we have performed the detailed study of magnetic behavior of several high-quality single crystals. Single crystals of $Pr_{0.6}Ca_{0.4}MnO_3$ are produced by the floating zone method and the samples presented in this paper were cut from the same rod. The details about the sample preparation and characterization can be found in Ref. 17. Magnetization measurements are performed in "Quantum Design" MPMS [superconducting quantum interference device (SQUID)] and PPMS (ac susceptibility and vibrating sample magnetization). Due to the highly nonlinear response at low temperatures, and in order to obtain the "virgin" curves, the sample

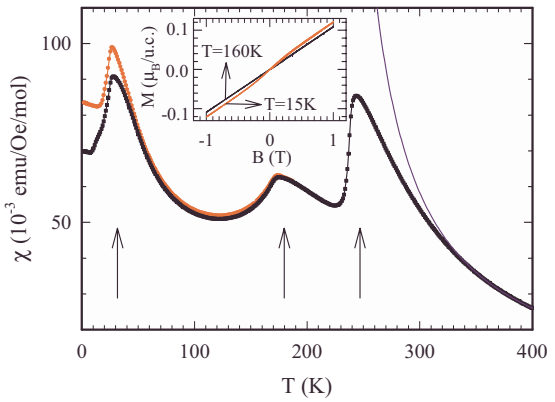

FIG. 1. (Color online) Temperature dependence of magnetic susceptibility χ for ZFC (black squares) and FC (red circles). $B=100$ Oe. Blue line is based on the Curie-Weiss fit to the region $350<T<400$ K. Arrows denote three AF-like transitions. Inset shows the field dependence of magnetization at $T=15$ and 160 K.

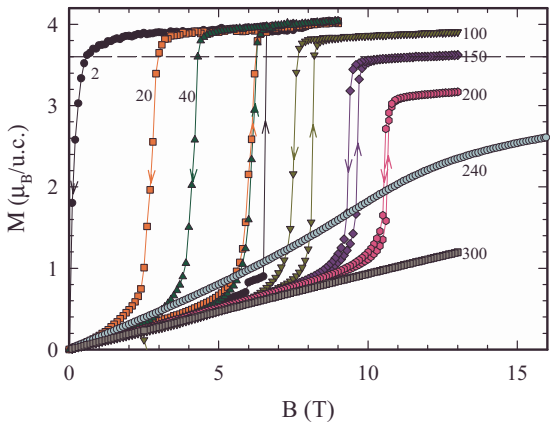

FIG. 2. (Color online) Magnetization M in Bohr magnetons per unit cell versus magnetic field B. Arrows denote the direction of field ramp. Numbers aside the curves indicate the temperature. $T=2$ (black circles), 20 (red squares), 40 (green triangles—up), 100 (dark-yellow triangles-down), 150 (blue diamonds), 200 (pink hexagons), 240 (cyan circles), and 300 K (gray squares). Broken line is the theoretically expected $M=3.6\mu_B$.

was heated to $T=260$ K after each magnetic cycle at low temperatures. Resistivity measurements are done in Quantum Design PPMS system.

II. RESULTS AND DISCUSSION

Figure 1 shows the temperature dependence of magnetic susceptibility $\chi(T)$ of the $Pr_{0.6}Ca_{0.4}MnO_3$ single crystal. Black circles and red squares stand for the zero-field-cooled (ZFC) and field-cooled (FC) (cooling with $B=100$ Oe) measurements. Magnetic field is 100 Oe. The arrows point to the three antiferromagneticlike transitions, and the line is a Curie-Weiss fit to the high-temperature ($T>350$ K) region. The transition at $T_{CO}=235$ K is usually assigned as the CO transition[7] and we shall label it in this way throughout this paper. Nevertheless, and as already mentioned in Sec. I, this transition is also interpreted as the onset of Zener-polaron ordering.[17] The magnetic susceptibility at high temperatures ($T>350$ K) is driven by ferromagnetic interactions as indicated by the Curie-Weiss fit $\chi \propto 1/(T-T_P)$ (blue line) that yields a positive $T_P=220$ K. In spite of these high-temperature ferromagnetic correlations, antiferromagnetism prevails at $T<235$ K. Still, FM correlations persist even at lower temperatures which can be seen in the subsequent increase in the susceptibility. The competition between FM and AF correlations leads to two additional AF transitions at $T_2=T_N=175$ K and $T_3=27$ K. The $T_3=27$ K transition is usually assigned as the onset to canted antiferromagnetism,[6] although T_2 was initially also reported to be a CAF transition.[9,20] Nevertheless, our $Pr_{0.6}Ca_{0.4}MnO_3$ sample is completely antiferromagentic in the almost entire temperature range. In the inset of Fig. 1 we show the low-field ($B<1$ T) magnetization versus magnetic field at $T=160$ and 15 K. At $T=160$ K, even at the smallest fields one cannot detect any trace of ferromagnetism. Only as $T\rightarrow 27$ K do the FM correlations grow stronger, and a trace of FM signal can be detected in the region $15<T<40$ K. This FM signal could correspond to less than 0.5% of the sample but probably indeed represents a minor canting of AF spins. In spite of this minor canting, the $T_3=27$ K transition in our material is predominantly (>99.5%) an AF transition. Around $T=T_3=27$ K (actually, in Fig. 1 below 40 K) the ZFC and FC susceptibilities differ considerably so this transition could be compatible with the phenomenology for the spin-glass transition. However, if the cooling is done in higher magnetic field ($B>100$ Oe) or if the magnetic field is cycled to larger values at $T<27$ K, the difference of ZFC and FC measurements (both in $B=100$ Oe) persists up to $T=170$ K, becoming colossal (orders of magnitude) at low temperatures. Thus, the difference between the ZFC and FC susceptibilities seems to be unrelated to the $T_3=27$ K transitions.

It is interesting to note that the temperature of the third AF transition coincides with temperatures of AF ordering of Pr ions. It is known that praseodymium ions in oxides generally order antiferromagnetically at $T\approx 30$ K.[21] Thus, it might be that the AF correlations of Pr ions at $T\approx 30$ K overcome the weak FM correlations of Mn ions resulting in the third AF transition. The magnetic coupling between Mn and Pr ions is already reported in $Pr_{0.7}Ca_{0.3}MnO_3$ ($x=0.3$). In this compound the long-range FM order of Mn ions occurs at $T\approx 130$ K and FM ordering of Pr^{3+} ions is observed at $T\approx 60$ K.[22] On the contrary, in our antiferromagnetic matrix ($x=0.4$) Pr ions probably order AF, as it occurs in praseodymium oxides.[21]

Figure 2 shows the hysteresis loops (just one quadrant) of magnetization versus field for one set of temperatures. Before each $M(B)$ curve the temperature is raised to $T=260$ K in order to erase the remnant magnetization after each field cycle. In Fig. 2 the magnetic field is swept: $B=0\rightarrow 9\rightarrow 0$ T. At all temperatures the initial ($0<B<2-3$ T) $M(B)$ curves are linear with no hysteresis. At sufficiently high magnetic fields ($B_C>5$ T) $Pr_{0.6}Ca_{0.4}MnO_3$ exhibits a first-order transition from the low-temperature AF state into the ferromagnetic state. On lowering the field, the ferromagnetism persists to lower fields

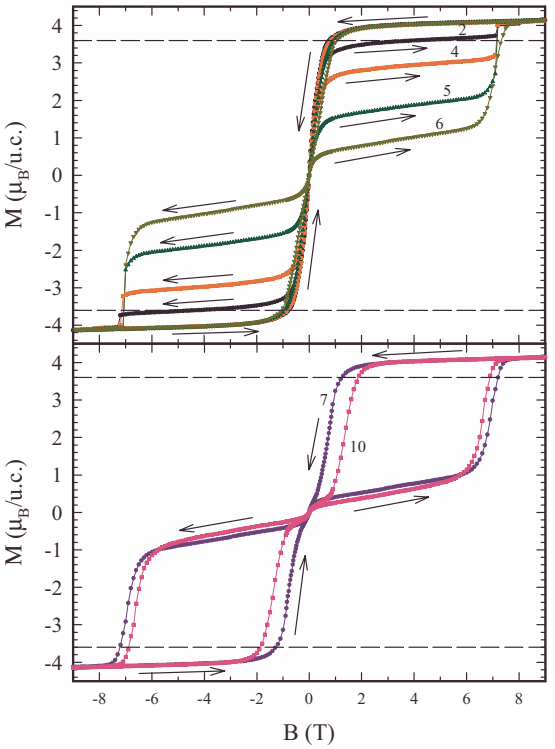

FIG. 3. (Color online) Magnetization M versus magnetic field B from magnetic cycles $B=9\rightarrow-9\rightarrow9$ T. Arrows denote the direction of field ramp. (a) $T=2$ (black circles), 4 (red squares), 5 (green triangles—up), and 6 K (yellow triangles-down). (b) $T=7$ (blue circles) and 10 K (pink squares). Broken line is the theoretically expected $M=3.6\mu_B$.

$(B_{C'})$, resulting in the pronounced hysteresis. The magnetic field-induced ferromagnetic (FIFM) transitions persist up to $T=225$ K$\approx T_{CO}$, i.e., much higher than $T=T_N=175$ K. The magnetic first-order transitions shown in Fig. 2 are reported by Tokunaga *et al.*[23] in similar systems $(Pr_{1-x}Ca_xMnO_3; x=0.45-0.5)$. Our system $(x=0.4)$ is different such that at low temperatures $(T=2$ K in Fig. 2) the FIFM persists down to $B\rightarrow0$ T.

Figure 3 shows the full hysteresis loops at temperatures $T\leq10$ K. The arrows denote the direction of B sweep. All the curves are $B=9\rightarrow-9\rightarrow9$ T cycles. One can see that the sample at $T\leq6$ K, once being in the FIFM state, remains ferromagnetic down to very low fields (the magnetization drops linearly and sharply from M_S to 0). We note that the sample is not superparamagnetic since $M(B)$ curves do not scale as $M(B/T)$. On reversing the field, the ferromagnetic moment reverses its sign but the reached saturation value M_S^* is lower than in the complete FIFM state $(M_S^*<M_S)$. Finally, at $B=\pm B_C$ the sample recovers full ferromagnetism. From our magnetization measurements it is difficult to assess the origin of this persistent fractional FM. It might be that the FM state persists only in one fraction of the sample; this would then present the macroscopic evidence of FM and AF phase separations in $Pr_{0.6}Ca_{0.4}MnO_3$. However, as shown in the inset of Fig. 1, we do not detect separated FM and AF phases in our sample, in accordance with Ref. 10. Therefore, more likely is that upon lowering the field, the spins flip from a FM to an incomplete AF orientation, resulting in a canted AF state with the net ferromagnetic moment.

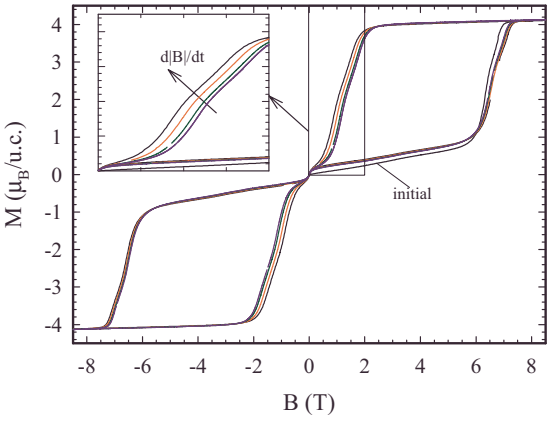

FIG. 4. (Color online) Magnetization M versus magnetic field B for different ramping rates of magnetic field: 130 (black), 50 (red), 20 (green), and 12 Oe/s (blue). Inset shows the enlarged portion of the main figure as indicated by the frame. In the inset, the ramping speed increases from right to left. $T=10$ K.

Increasing the temperature to $T>6$ K $(T=7-10$ K) [Fig. 3(b)] the FIFM state weakens. Indeed it disappears at fields higher than those at low temperatures yielding a new state responsible for the hump around $B=0$ T. This is not observed for temperatures $T>20$ K. This means that, although the FIFM state turns off at $B>0$, one small FM component remains even at $B=0$. In order to explore if this persistent FIFM is a reminiscence of some glassy behavior, we have checked if it is time dependent. Figure 4 shows the $M(B)$ cycles at $T=10$ K for various ramping rates of magnetic field. Four ramping rates are shown [for the cycles $(B=8.5\rightarrow-8.5\rightarrow8.5$ T)]: 130, 50, 20, and 12 Oe/s. Initial ramp $B=0\rightarrow8.5$ T (black line with a different shape when comparing to the other cycles) is made with 130 Oe/s. Data in Fig. 4 correspond to another single crystal from the same rod, and the results are identical to the $T=10$ K curve in Fig. 3. It can be seen that the ramping rate enlarges slightly the hysteresis width, as is the case for these metamagnetic transitions at all temperatures. However, the main features of these $T=10$ K cycles remain the same: (a) $B_C\approx6.5$ T, (b) there is a small FM part of the curve (coming out of $B=0$ T) just below $B=0.2-0.4$ T, and (c) all the returning curves (lowering the field toward $B=0$ T) collapse in the same $B=0.2-0.4$ T point.

From the above we conclude that the persistent FIFM depends only on the temperature and that the time effects due to different ramping rates are common to FIFM at all temperatures (up to $T=230$ K) and do not correlate to a glassy behavior in this particular temperature range. In Fig. 5 we have plotted the ratio of fractional saturation magnetization $[M_S^*(T)/M_S(T)]$ as a function of temperature. The values of M_S^* (black diamonds) are taken from Fig. 3 as the extrapolation $M(B=0)$ of the ferromagnetic part of $M(B)$ loops when B increases $(d|B|/dt>0)$. M_S^* drops sharply at $T\approx6$ K and disappears completely at $T=15$ K. We find that this temperature variation in M_S^* is dependent on the hole concentration "x." We have observed the same curves in all samples cut from the same rod, but in the similar system $(x=0.375)$ (red

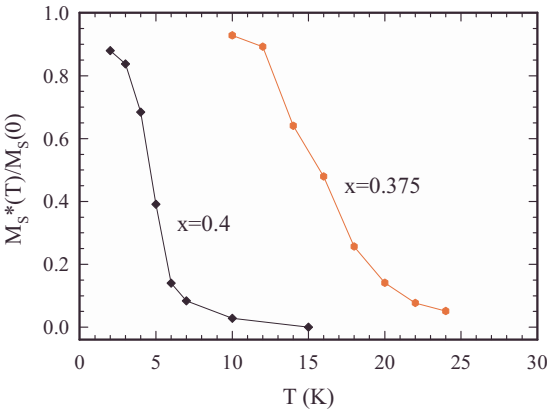

FIG. 5. (Color online) Fractional saturation magnetization M_S^* normalized to the full saturation M_S as a function of temperature for $Pr_{1-x}Ca_xMnO_3$. Line is a guide to the eyes.

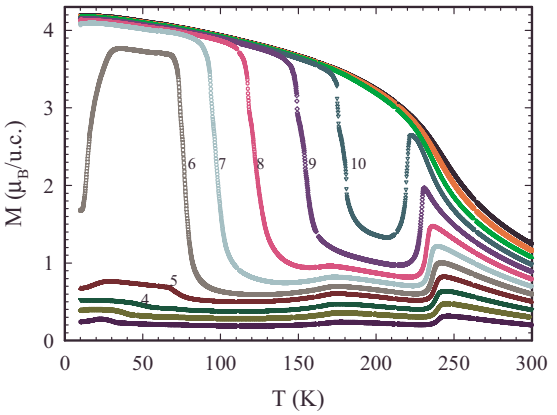

FIG. 7. (Color online) Magnetization M versus temperature T for fixed fields between $B=13$ (upper curve) and 2 T (lowest curve). $\Delta B=1$ T between each curve. Numbers close to some of the curves correspond to their values of B.

circles) we have observed FM part even at $T=20$ K. This increase in persistent FIFM in $x=0.375$ sample is consistent with the stronger FM character of $Pr_{1-x}Ca_xMnO_3$ material as $x\rightarrow 0.3$.

The $T=27$ K AF transition in Fig. 1 draws another consequence in the regimes of high magnetic fields. The virgin $M(B)$ curves (those increasing from $B=0$ in Fig. 2) show that the critical field B_C for the onset of ferromagnetism has a minimum at $T\approx 30$ K. This indicates that the $T=27$ K is just the temperature where the ferromagnetic correlation are the strongest compared to the antiferromagnetic ones. At 27 K the system undergoes a new AF transition, and a stronger magnetic field is again necessary to overturn the spins into the FM order. The dependence of B_C on temperature is shown in the phase diagram in Fig. 6 by green diamonds. Note a sharp overturn at $T=30$ K. The same phase boundary,

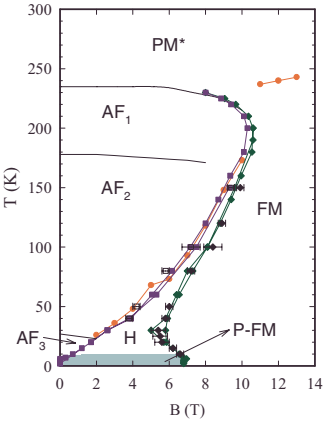

FIG. 6. (Color online) T-B phase diagram. Black lines are the three AF transitions as deduced from Fig. 7. Green diamonds are FIFM transition fields B_C as deduced from Figs. 3 and 4 when $d|B|/dt>0$. Blue squares are transition fields $B_{C'}$ when $d|B|/dt<0$ from the same figures. Red circles are FIFM transition temperatures $T_{C'}$ for the fixed field, taken from Fig. 7. Black diamonds and empty squares are the FIFM transitions B_C and $B_{C'}$ taken from our resistivity measurements $R(B)$. Shadowed region is the region of persistent ferromagnetism. Acronyms of the phases are defined in text.

including the 30 K overturn, is observed from the onset of CMR in our resistivity measurements (black diamonds), indicating that CMR in $Pr_{1-x}Ca_xMnO_3$ coincides with the onset of long-range FM order. The same overturn was reported in the phase diagram by Tomioka *et al.*[6] and it was suggested to be a consequence of "a decrease in the thermal fluctuation effect on the first-order phase transition." Here we propose that it is related to the "27 K" AF transition as stated above. When the magnetic field is lowered, FIFM state persists to lower fields $B_{C'}$ (blue squares), resulting in the large hysteresis area labeled as "H" in Fig. 6. Empty squares denote $B_{C'}$ from our resistivity measurements (not shown here) that coincide with those from magnetic measurements. In the H phase the shadowed (cyan) region, labeled as P-FM, is the region of persistent ferromagnetism as defined in Figs. 3–5. Note that the phase diagram in Fig. 6 corresponds to the $x=0.4$ compound, while in that of $x=0.375$ the P-FM region exists up to 20 K. Outside of this hysteretic region we have pure FM and AF phases. At temperatures higher than 240 K, PM* denotes the paramagnetic phase.

Another way to study the complex magnetic properties of such system is to sweep the temperature at a fixed magnetic field. Experimental steps are the following: (a) sample is cooled in the zero magnetic field to $T=10$ K, (b) magnetic field is raised to a fixed value, (c) the sample is heated up to 300 K, and (d) field is turned off. The result of this experiment is shown in Fig. 7. The curves show the temperature dependence of magnetization $M(T)$ in Bohr magnetons per unit cell for fixed fields between $B=13$ T (uppermost curve, black) to $B=2$ T (lowest curve, blue) with $\Delta B=1$ T between each curve. The rich structure of these curves will give us the rest of the points in the phase diagram (Fig. 6). The temperature of the highest AF transition T_{CO} decreases by almost 10% when B increases up to $B=10$ T. The field of 11 T overcomes completely the inherent antiferromagnetism, and the system is completely ferromagnetic below T_{CO}. The temperature of second AF transition $[T_N(B=0)=175$ K] decreases in magnetic field by just 4% until it is not detectable at $B=9$ T. The third AF transition at $T=27$ K is well pronounced just at small fields. These three transitions are rep-

resented by black lines in Fig. 6. It is interesting to note that the $T=175$ K AF transition has no major impact in the phase diagram.

Red circles in Fig. 6 represent the ferromagnetic transition temperature $T_{C'}$ as deduced from Fig. 7. At $B \geq 11$ T $T_{C'}$ is defined as the inflection point in the $M(T)$ curve. For $B<11$ T, $T_{C'}$ is defined as the temperature where $M(T)$ curve decreases sharply $(-dM/dT=\max)$ from FM to AF state. As expected, $T_{C'}$ data correspond precisely to the $B_{C'}$ data (blue squares), which means that they depict the same property. The most intriguing in Fig. 7 is the sudden increase in $M(6$ T) between $T=10$ and 30 K. Actually, all $M(T)$ curves for $B<7$ T start with the lower value at $T=10$ K and then raise to a plateaulike value. This interesting feature is merely the fact that at these particular fields, the (ferro)magnetism is not complete, as the system is on the feet of the large increase in $M(B)$ (Fig. 2). For example, at $T=10$ K, increasing the field to $B=6$ T brings the material just below the FIFM transition $[B_C(10\ \text{K})=6.5\ \text{T}]$. The increase in temperature then increases the magnetization toward M_S since B_C decreases toward $T \approx 30$ K. In a certain region of temperature (30–70 K) the system is in FIFM state. With a further increase in temperature, the B_C becomes larger than 6 T and M falls again—this temperature is the above-labeled $T_{C'}$. At fields lower than B_C ($B=2$, 3, and 4 T) the anomaly is much smaller and is finally reduced to the 27 K anomaly observed in Fig. 1.

The $M(T)$ data presented in Fig. 7 are rather similar to the $M(T)$ data observed in $La_{0.215}Pr_{0.41}Ca_{3/8}MnO_3$ (LPCMO).[24] In the latter case it was reported that $M(T)$ data reveal a phase boundary not detectable in usual $M(B)$ measurements. The low-temperature increase in $M(T)$ (similar to the $B=6$ T trace in Fig. 7) was interpreted as the crossing from the low-temperature strain-glass phase to the strain-liquid phase.[24] Their complex system (three different ions on the perovskite A site: La, Pr, and Ca) is considered to be a prototype system for percolative phase separation.[4] The two competing phases were considered to be FM metallic and CO/AF insulating phases, and the freezing from dynamic to static phase-separated state was labeled as the "strain glass."[24] The border between the strain-glass and strain-liquid phases was determined by both transport and magnetization measurements. In the magnetization measurements, this border is defined as the increase in $M(T)$ when raising the temperature—similar to the case of $M(T, B=6$ T) in Fig. 7. In the case of $Pr_{0.6}Ca_{0.4}MnO_3$ we have seen that the decrease in $M(T, B=6$ T) in Fig. 7 at $T<30$ K is a direct consequence of the minimum of B_C around $T=30$ K which, in return, is the consequence of strongest FM correlations at this temperature. Also, contrary to Ref. 24 we were not able to deduce a convincing temperature dependence of this "glass-liquid" border; dM/dT for $T<30$ K is rather small and ambiguous when $B<6$ T. Therefore, from our experiment we can only conclude that the third AF ordering at $T=27$ K causes the low-temperature anomaly of $M(T)$ (Fig. 7) ($B=6$ T trace). Nevertheless, it is worth noting that the same cause could produce similar effects in LPCMO. Although the LPCMO system is more complex than PCMO ($Pr_{1-x}Ca_xMnO_3$), the AF ordering on the Pr site in LPCMO could reinforce locally the insulating AF state. As $T \to 0$, this AF order gets stronger and a larger magnetic field is necessary to overturn it into the metallic FM state.

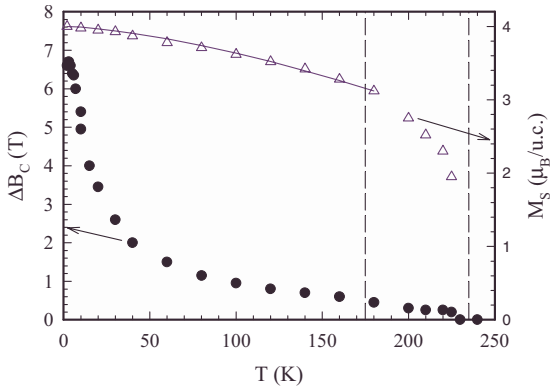

FIG. 8. (Color online) Hysteresis width $\Delta B_C = B_C - B_{C'}$ (black circles, left axis) and the saturation magnetization M_S (triangles, right axis) as a function of temperature. Vertical broken lines indicate $T_N=175$ K and $T_{CO}=235$ K. Line is a fit to Bloch $T^{3/2}$ law.

Finally, we want to stress that the FIFM, corresponding to the flipping of AF into FM order, persists up to $T_{CO}=235$ K. In Fig. 8 we plot the hysteresis width ΔB_C of the metamagnetic transitions (FIFM state) as a function of temperature. $\Delta B_C = B_C - B_{C'}$ is taken at the half height of the FIFM transitions. One can observe the strong increase in ΔB_C below 30 K and the disappearance of hysteresis $(\Delta B_C \to 0)$ at $T=230$ K. Therefore, the first-order magnetic transitions do correspond to a complete long-range AF order present until $T=230<235\ \text{K}=T_{CO}$. The existence of the first-order FIFM transitions up to T_{CO} is well known and reported in Refs. 6 and 22. Here we want to stress out that this indicates the equivalence of the magnetic states at $T<T_N=175$ K and $175<T<235\ \text{K}=T_{CO}$. This then questions the widely accepted picture of charge order as the origin of T_{CO} anomaly and suggests the existence of an antiferromagnetic order also in the $175<T<235$ K range. In the same graph we plot the "saturation magnetization" M_S of FIFM states (right axis, triangles). M_S is taken as the interception on "y" axis of the linear part of $M(B)$ in the FIFM state. At $T=2$ K M_S reaches the value of $M_S=3.9\mu_B$ per cell unit. This value is higher than expected if just Mn^{3+} and Mn^{4+} ions order ferromagnetically and probably includes the (canted) ferromagnetic contribution of Pr^{3+} ions. What is more surprising is that the temperature behavior of M_S follows the $T^{3/2}$ rule, as if the magnon dispersion indeed decays the FIFM state. This indicates that the FM contribution of Pr ions remains locked within the Mn lattice to at least $T_N=175$ K.

III. CONCLUSION

We have reported on the magnetism in $Pr_{0.6}Ca_{0.4}MnO_3$ which can be separated into the spontaneous antiferromagnetism $(B<B_C)$ and induced ferromagnetism (after magnetic transitions at B_C). Regarding spontaneous magnetic order, three successive AF transitions result as a consequence of the strong competition between FM and AF correlations. After

each of these transitions, no inhomogeneities (mixture with FM or CAF phases) are found in the sample. At sufficiently high magnetic fields ($B > B_C$) the AF order is flipped into the FM one. This first-order (hysteretic) transition is observed up to $T=225$ K $\approx T_{CO}$ which supports the assignment of first transition at $T_{CO}=235$ K as an AF transition. The hysteresis width increases with decreasing temperature, yielding to persistent FIFM states as $B \to 0$ at $T < 10$ K. At these temperatures, as $|B|$ increases again, the saturation magnetization M_S^* of persistent FIFM states is smaller than the observed total M_S and decreases with temperature. We interpret this fractional M_S^* as a switching from the complete FM into the incomplete ferro state, i.e., into a CAF state. The total M_S of FIFM state at low temperatures reaches $3.9\mu_B$ per cell unit, indicating the CAF contribution of Pr^{3+} ions. When $B > B_C$, the canting of AF alignment of Pr ions increases and raises the magnetization, as can be seen from the finite slope of $M(B)$ in FIFM state (Figs. 2–4). Nevertheless, when $B=$const the total magnetization of FIFM state, including CAF of Pr ions, decays upon the Bloch $T^{3/2}$ law up to $T=180$ K (Figs. 7 and 8). Finally, we note that the $T_3=27$ K AF transition has a pronounced impact on FIFM transitions, resulting in a minimum of transition field B_C around 27 K. This in turn produces an anomaly in $M(T)$ (Fig. 7) similar to the one that has been interpreted as the strain-glass transition in a phase-separated $La_{0.215}Pr_{0.41}Ca_{3/8}MnO_3$. We interpret the same $M(T)$ anomaly in $Pr_{0.6}Ca_{0.4}MnO_3$ as a consequence of the 27 K AF transition driven by Pr^{3+} AF ordering.

ACKNOWLEDGMENTS

We wish to thank L. Pinsard-Gaudart for providing us a high-quality sample. We acknowledge financial support from Ministerio de Educacion y Cincia (Grants No. MAT2005-06024-C02-01 and No. MAT2006-01004). One of us (N.B.) acknowledges Ramon and Cajal program from Ministerio de Educacion y Ciencia in Spain.

*biskup@icmm.csic.es

[1] E. Dagotto, Science **309**, 257 (2005).
[2] For the review of this subject, see E. Dagotto, T. Hotta, and A. Moreo, Phys. Rep. **344**, 1 (2001).
[3] E. Dagotto, New J. Phys. **7**, 67 (2005).
[4] M. Uehara, S. Mori, C. H. Chen, and S.-W. Cheong, Nature (London) **399**, 560 (1999).
[5] M. Fäth, S. Freisem, A. A. Menovsky, Y. Tomioka, J. Aarts, and J. A. Mydosh, Science **285**, 1540 (1999).
[6] Y. Tomioka, A. Asamitsu, H. Kuwahara, Y. Moritomo, and Y. Tokura, Phys. Rev. B **53**, R1689 (1996).
[7] Z. Jirák, S. Krupička, Z. Šimša, M. Dlouhá, and S. Vratislav, J. Magn. Magn. Mater. **53**, 153 (1985).
[8] H. Yoshizawa, H. Kawano, Y. Tomioka, and Y. Tokura, Phys. Rev. B **52**, R13145 (1995).
[9] M. R. Lees, J. Barratt, G. Balakrishnan, D. McK. Paul, and M. Yethiraj, Phys. Rev. B **52**, R14303 (1995).
[10] P. G. Radaelli, R. M. Ibberson, S.-W. Cheong, and J. F. Mitchell, Physica B **276-278**, 551 (2000).
[11] P. G. Radaelli, R. M. Ibberson, D. N. Argyriou, H. Casalta, K. H. Andersen, S.-W. Cheong, and J. F. Mitchell, Phys. Rev. B **63**, 172419 (2001).
[12] P. G. Radaelli, D. E. Cox, M. Marezio, and S.-W. Cheong, Phys. Rev. B **55**, 3015 (1997).
[13] T. Hotta, Y. Takada, H. Koizumi, and E. Dagotto, Phys. Rev. Lett. **84**, 2477 (2000).
[14] J. Tao and J. M. Zuo, Phys. Rev. B **69**, 180404(R) (2004).
[15] M. Coey, Nature (London) **430**, 155 (2004).
[16] J. C. Loudon, S. Cox, A. J. Williams, J. P. Attfield, P. B. Littlewood, P. A. Midgley, and N. D. Mathur, Phys. Rev. Lett. **94**, 097202 (2005).
[17] A. Daoud-Aladine, J. Rodríguez-Carvajal, L. Pinsard-Gaudart, M. T. Fernández-Díaz, and A. Revcolevschi, Phys. Rev. Lett. **89**, 097205 (2002).
[18] L. Wu, R. F. Klie, Y. Zhu, and Ch. Jooss, Phys. Rev. B **76**, 174210 (2007).
[19] A. M. L. Lopes, J. P. Araújo, V. S. Amaral, J. G. Correia, Y. Tomioka, and Y. Tokura, Phys. Rev. Lett. **100**, 155702 (2008).
[20] A. Maignan, C. Martin, F. Damay, and B. Raveau, Z. Phys. B: Condens. Matter **104**, 21 (1997).
[21] B. D. Cullity, *Introduction to Magnetic Materials* (Addison-Wesley, Menlo Park, CA, 1972); S. Kern, J. Chem. Phys. **40**, 208 (1964); J. B. MacChesney, H. J. Williams, R. C. Sherwood, and J. F. Potter, *ibid.* **41**, 3177 (1964).
[22] D. E. Cox, P. G. Radaelli, M. Marezio, and S. W. Cheong, Phys. Rev. B **57**, 3305 (1998).
[23] M. Tokunaga, N. Miura, Y. Tomioka, and Y. Tokura, Phys. Rev. B **57**, 5259 (1998).
[24] P. A. Sharma, S. B. Kim, T. Y. Koo, S. Guha, and S.-W. Cheong, Phys. Rev. B **71**, 224416 (2005).